

## Light Scattering Study of Ionomers in Solution. 4. Angular Measurements of Sulfonated Polystyrene Ionomers in a Polar Solvent (Dimethylformamide)

Jeffrey Bodycomb and Masanori Hara\*

Department of Mechanics and Materials Science, Rutgers, The State University of New Jersey, Piscataway, New Jersey 08855-0909

Received June 24, 1994\*

**ABSTRACT:** The salt-free polyelectrolyte behavior of random ionomers, i.e., partially sulfonated polystyrene (SPS) (Na salt: MW = 400 000) having less than 5 mol % of ionic groups, dissolved in an aprotic polar solvent, dimethylformamide (DMF), was studied by angular light scattering measurements. At low ionomer concentration, "abnormal" Zimm plots, showing negative slopes in reciprocal reduced scattered intensity vs scattering vector curves, are observed. These effects arise because the scattering is dominated by external interference arising from strong electrostatic interactions between charged ionomer chains. The behavior can be explained by using general relations derived by extending the approach of Doty and Steiner. As concentration is increased, these slopes become less negative and eventually become positive with some curvatures at small angles, which suggests the existence of large-scale "heterogeneities" in the solution. As ion content is increased, the initial slopes become more negative at low concentration and become more positive at higher concentration. Such behavior is suppressed upon addition of simple salts, suggesting that the observed behavior is ionic in nature. The angular light scattering experiments confirm previous conclusions drawn from low-angle light scattering experiments on the salt-free polyelectrolyte behavior of ionomers in polar solvent. The results also seem to be consistent with the speculation about the presence of large "heterogeneities" in salt-free polyelectrolyte solutions, suggested by some dynamic light scattering experiments.

### Introduction

The solution behavior of polyelectrolytes with added salts is well explained;<sup>1,2</sup> the solution is treated like a neutral polymer in a "very good" solvent by using excluded volume theory<sup>3</sup> and scaling theory,<sup>4</sup> originally developed for understanding the solution behavior of neutral polymers. However, the solution behavior of salt-free polyelectrolyte solutions is still not well understood;<sup>2</sup> there still exist controversies about the structure of salt-free solution and the causes of the characteristic behavior of these solutions. One of the reasons is the difficulty in obtaining reliable data for salt-free aqueous polyelectrolyte solutions, since these solutions are more difficult to handle than their added-salt counterparts. For example, while light scattering techniques have been widely used to obtain useful information for added-salt systems,<sup>1</sup> little work has been reported for salt-free solutions. This is because the excess scattered intensity is very small for salt-free solutions at very low concentration, needed to obtain basic information.

Recently, it has been shown that ionomers dissolved in a polar solvent can be used as good model systems to study the characteristic behavior of salt-free polyelectrolyte solutions.<sup>5</sup> Ionomers are a class of ion-containing polymers with a small number of ionic groups, up to 10–15 mol %, attached to nonionic backbone chains.<sup>6–8</sup> It is now well established that ionomers show two types of behavior in solution depending mainly on the polarity of the solvent:<sup>9</sup> in low-polarity solvents, such as toluene ( $\epsilon = 2.4$ ), aggregation behavior due to dipolar attraction is observed,<sup>10,11</sup> and in polar solvents, such as DMF ( $\epsilon = 37$ ), polyelectrolyte behavior due to electrostatic interactions is observed;<sup>12</sup> here,  $\epsilon$  is the dielectric

constant of the solvent. However, it should be cautioned that the term *ionomer* is usually more connected with aggregation behavior, since much of the ionomer work has been focused on the structure and properties of ionomer solids.<sup>6–8</sup> In the solid state, ionic groups are dispersed in a medium of low dielectric constant, e.g., polyethylene or polystyrene ( $\epsilon = 2.5$ ), where counterions are strongly bound to fixed ions and resulting dipolar attraction leads to the formation of ionic aggregates. In this work, we will focus entirely on the *polyelectrolyte behavior* of ionomers in a polar solvent, where many of the counterions are dissociated.<sup>12</sup>

In polar solvents, it has been demonstrated that ionomers show polyelectrolyte behavior. The reduced viscosity of ionomers increases markedly with decreasing polymer concentration.<sup>9</sup> This behavior, characteristic of polyelectrolyte solutions, can be suppressed by the addition of simple salts.<sup>12,14</sup> Low-angle light scattering data from ionomer solutions also show a typical polyelectrolyte behavior: a marked decrease in scattered intensity with increasing ionomer concentration.<sup>13–16</sup> Again, such behavior can be suppressed by adding simple salts.<sup>14</sup> It is interesting to note that telechelic ionomers, which have only one or two ionic groups attached to the chain ends, also show similar polyelectrolyte behavior, observed by viscosity and low-angle light scattering experiments.<sup>17,18</sup> This indicates the importance of intermolecular electrostatic interactions in the development of this characteristic behavior, since no intramolecular electrostatic interactions are available for monofunctional telechelic ionomers. Small-angle neutron scattering (SANS) and small-angle X-ray scattering (SAXS) on ionomers in polar solvents have also shown the typical scattering behavior of polyelectrolytes in aqueous solution:<sup>19–21</sup> a broad single peak in scattered intensity vs scattering vector is observed. In addition, dynamic light scattering<sup>15,22,23</sup> and osmotic pressure measurements<sup>12</sup> for ionomer solutions gener-

\* To whom all correspondence should be addressed.

† Abstract published in *Advance ACS Abstracts*, November 1, 1994.

ally show similar behavior to that of polyelectrolyte solutions. The equivalent conductance decreases significantly with increasing ionomer concentration, as typically observed for polyelectrolyte solutions, due to counterion binding to polyion chains, in contrast to simple salt analogues, which show slight decrease with concentration.<sup>24</sup> It should be stressed that all of these observations for ionomer solutions parallel those from polyelectrolyte/water systems.<sup>25–28</sup> A recent review on the behavior of polyelectrolytes and ionomers in non-aqueous solution is available.<sup>5</sup>

In contrast to solutions of neutral polymers that have only relatively weak, short-range interactions on the one hand, and polyelectrolytes with 100 mol % ionic groups that have very strong, long-range electrostatic interactions on the other, ionomers are considered to be an intermediate system.<sup>5</sup> Because of a smaller number of charges in ionomer chains compared with polyelectrolytes, the reduction in scattering power due to destructive interference is much smaller. For example, the excess scattered intensity from SPS ionomers dissolved in DMF is  $(1-20) \times 10^{-6} \text{ cm}^{-1}$ ,<sup>13</sup> while that from sodium polymethacrylate or sodium poly(styrenesulfonate) with comparable molecular weight dissolved in water is  $(0.1-1) \times 10^6 \text{ cm}^{-1}$ .<sup>28,29</sup> If some foreign particles exist in solution, which may be the case even after careful optical clarification, their scattering contribution is not negligible compared with the scattering from polyelectrolyte molecules, which is very small. This effect is less serious for ionomer solutions because of the stronger scattering power of the solution. In addition, nonaqueous solvent, such as DMF, has a closer refractive index (1.43) than water (1.33) to that of many foreign particles (1.4–1.6);<sup>30a</sup> therefore, the scattering contribution from foreign particles is even smaller, since the scattering power is proportional to the square of the difference of refractive index between foreign particles and the solvent. Also, the scattering problem from the glass cell/solution interface is less serious, since the refractive index of DMF is much closer than water to that of the glass (e.g., 1.50). It should also be added that SPS ionomers seem to be more stable than poly(styrenesulfonate) presumably because of the smaller amounts of sulfonate groups in the SPS ionomers.<sup>30b</sup> Finally, the use of aprotic solvent prevents problems associated with aqueous solution, such as autodissociation of the solvent (water).<sup>2</sup>

In this work, we extend our previous studies, conducted by low-angle scattering on the salt-free polyelectrolyte behavior of random ionomer solutions (SPS ionomer in DMF), to include angular light scattering experiments at wide angles. The SPS ionomers, in which ionic groups are randomly distributed along the backbone chains, have been used extensively for studying solution behavior.<sup>5</sup> We previously used these ionomers for viscosity,<sup>14,31,32</sup> low-angle light scattering,<sup>13,16</sup> and dynamic light scattering<sup>22,23</sup> experiments. The angular measurements would allow us to discuss the solution behavior of ionomers in terms of the structure factor, which gives information on the structure of the solution, in addition to the low-angle scattering results, which gives information on thermodynamic parameters. The purpose of the present work is to compare some of our results with those reported for salt-free polyelectrolyte solutions by using light scattering techniques and to obtain new information concerning characteristic salt-free polyelectrolyte behavior by using ionomer solutions.

**Table 1. Molecular Characteristics of Polymers and the Refractive Index Increment,  $dn/dc$ , of the Polymers in DMF**

$M_w^a$	$M_w/M_n^b$	ion content <sup>c</sup> (mol %)	$dn/dc^d$
$4.0 \times 10^5$	1.06	0	0.165
		1.9	0.161
		2.7	0.168
		4.6	0.171

<sup>a</sup> Determined by low-angle light scattering measurements.

<sup>b</sup> Data from Pressure Chemical. <sup>c</sup> Determined by titration. <sup>d</sup> Determined by differential refractometer.

## Experimental Methods

**Materials.** Lightly sulfonated polystyrene (SPS) was prepared by sulfonation of polystyrene with a sulfonating agent, acetyl sulfate.<sup>33</sup> The starting polymer was polystyrene (PS) (MW = 400 000) with a narrow molecular weight distribution ( $M_w/M_n = 1.06$ ) (Pressure Chemical). After the reaction was terminated by adding methanol, polymer (acid form) was recovered by steam stripping in boiling water. The acid content of the copolymer samples was determined by titration of the sulfonic acid groups using a standard sodium hydroxide solution with phenolphthalein as an indicator in a solvent mixture, benzene/methanol (90/10 v/v). Acid copolymers were then converted to ionomers (sodium salt) by adding a calculated amount of methanolic sodium hydroxide. All the polymers were obtained in a powder form by freeze-drying, followed by vacuum drying at room temperature for at least 1 week. Details about the preparation and characterization of SPS polymers are described elsewhere.<sup>16,32</sup> The molecular characteristics of the polymer samples are summarized in Table 1. Sodium nitrate ( $\text{NaNO}_3$ ) (Fisher) was used as a simple salt, since  $\text{NaNO}_3$  has high solubility in DMF.

**Measurements.** Polymer solutions were prepared by dissolving the freeze-dried ionomer samples in DMF (Fisher: Spectranalyzed grade) under stirring overnight at room temperature to prepare a stock solution. The polymer was easily dissolved in DMF. Dilution of the stock solution was conducted inside a dust-free hood (Class 100K Hood: Laminare Co.) to avoid contamination by airborne dust.

Low-angle light scattering experiments were performed with a KMX-6 low-angle light scattering photometer (Chromatix) at a wavelength of 633 nm at  $25 \pm 0.5^\circ\text{C}$ . The effect of large dust particles was eliminated by using a flow cell. Since the absolute scattered intensity is directly calculated from the geometrical parameters and the ratio of radiant power, the usual calibration is unnecessary.<sup>34</sup> The specific refractive index increment,  $dn/dc$ , was measured at  $25 \pm 0.1^\circ\text{C}$  by a KMX-16 differential refractometer (Chromatix). The  $dn/dc$  values of ionomers and polystyrene in DMF are listed in Table 1. The optical clarification of the solutions was performed by filtration through 0.5 and 0.2  $\mu\text{m}$  filters (Millipore) with a constant flow rate using a syringe pump. The details concerning the low-angle light scattering experiments are described elsewhere.<sup>16</sup>

Angular light scattering measurements were performed with a BI-200SM photogoniometer (Brookhaven) with a 35 mW He-Ne laser (632.8 nm) and a BI-2030 digital correlator (Brookhaven). Each cylindrical sample cell with 24 mm diameter was cleaned for 2 h with a Thurmond type washing apparatus; this is a very effective method to remove dust particles.<sup>35</sup> The cell was mounted at the center of a vat filled with toluene (Fisher: Spectranalyzed grade) to match the refractive index of the glass cell to reduce problems, such as flare. The vat temperature, controlled by circulating ethylene glycol through tubes in the vat, was monitored via a thermocouple immersed in the index matching fluid surrounding the sample cell. The calibration of the goniometer was done for each measurement using the index matching fluid as a calibration standard, whose Rayleigh ratio is  $14.0 \times 10^{-6} \text{ cm}^{-1}$ .<sup>36</sup> The difference in the calibration constant between different runs was usually less than 1%.

A sample cell was first filled with filtered solvent (DMF), and intensity data were collected. This not only gave values

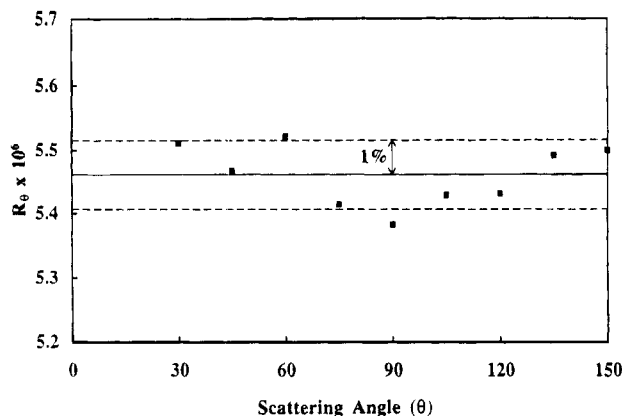


**Figure 1.** Reduced scattered intensity vs scattering angle for pure DMF.

for the background scattering but also was used to check the alignment of the instrument each time it was used. After this measurement, the cell was removed and cleaned again in the Thurmond apparatus. Then a stock solution was filtered into the scattering cell; subsequent solutions with lower concentrations were prepared by serial dilution in the scattering cell with filtered solvent, and the concentration was determined by weighing the scattering cell after each addition of the solvent. Optical clarification of solutions was performed by filtration through 0.5 and 0.2  $\mu\text{m}$  filters in succession in the dust-free hood. Scattered intensity was measured at each angle from 30 to 150° in 15° intervals. Since the flow cell system of the KMX-6 low-angle light scattering instrument allows us to remove scattering from dust as already described, the angular data extrapolated to 0° was compared with that from low-angle measurements to ensure that the angular data were free from the dust effect and thus reliable for further analysis.

**Standard Tests.** To ensure that the photogoniometer used for angular measurements was properly aligned and appropriate experimental procedure was followed, measurements on standards were performed. The first standard used was the pure solvent for checking the alignment of the light scattering instrument: the scattered intensity of the solvent in the scattering cell, after the volume correction of  $\sin \theta$ , should be independent of the scattering angle if the instrument is properly aligned. A plot of angular dependence of the scattered intensity from pure solvent showed a deviation from average value less than  $\pm 1\%$  for toluene. This test was done for DMF prior to each scattering experiment. An example of the plot of the scattered intensity against scattering angle for pure DMF is shown in Figure 1. The deviation from the average value is less than  $\pm 1.5\%$ , reflecting the proper alignment of the instrument.

The second standard used was polystyrene standard (MW = 400 000). The basic parameters obtained from a Zimm plot of polystyrene in toluene were in good agreement with the literature values.<sup>37</sup> The Zimm plot for polystyrene in DMF is shown in Figure 2: basic parameters obtained are a weight-average molecular weight,  $M$ , of  $3.92 \times 10^5$ , a radius of gyration,  $R_g$ , of 239 Å, and a second virial coefficient,  $A_2$ , of  $1.95 \times 10^{-4}$ . These measurements on polystyrene standards have demonstrated the reliability of our light scattering experiments. The results on DMF solutions were also used as a reference to compare with the results on ionomer solutions.

### Light Scattering Equations

Various forms of equations are used for analyzing light scattering data. Among the most general is one given by the following Zernicke-Prins equation.<sup>38</sup>

$$R_\theta = [KcMP(\theta)] \left[ 1 - \frac{N}{V} \int_0^\infty \{1 - \varrho(r)\} \frac{\sin(qr)}{qr} dv \right] \quad (1)$$

where  $R_\theta$  is the excess reduced scattered intensity at

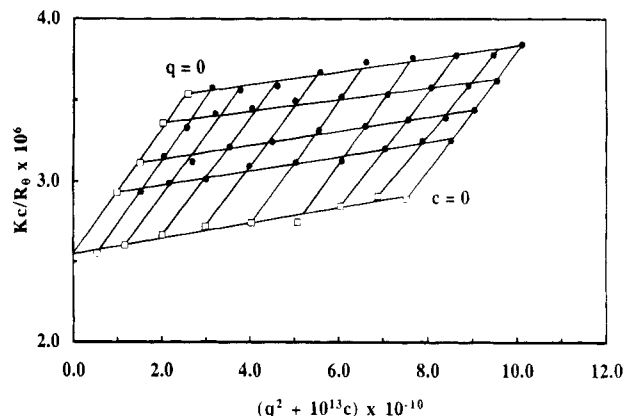


**Figure 2.** Zimm plot for polystyrene standard in DMF: closed symbols, experimental values; open symbols, extrapolated values.

angle  $\theta$  from the solution.  $K$  is the optical constant, defined by  $4\pi^2 n_0^2 (dn/dc)^2 / N_A \lambda_0^4$  for a polarized incident beam, where  $n_0$  is the refractive index of the solvent,  $dn/dc$  is the refractive index increment,  $N_A$  is Avogadro's number, and  $\lambda_0$  is the wavelength of the incident light in vacuo.  $c$  is the polymer concentration ( $\text{g}/\text{cm}^3$ ),  $M$  is the (weight-average) molecular weight, and  $P(\theta)$  is the particle (molecular) scattering factor.  $N$  is the number of molecules in the scattering volume,  $V$ ,  $\varrho(r)$  is the radial distribution function, and  $q$  is the magnitude of the scattering vector defined by  $q = (4\pi n / \lambda_0) \sin(\theta/2)$ . The first bracketed term in eq 1 represents the scattering from a single polymer chain, and the second bracketed term reflects the effect of external interference of light arising from intermolecular interactions.<sup>38</sup>

When the interactions between polymer chains are relatively weak, as is the case for neutral polymers at low concentrations, the external interference is small and the reciprocal reduced scattered intensity can be expressed in terms of a virial expansion<sup>3,39</sup>

$$\frac{Kc}{R_\theta} = \frac{1}{MP(\theta)} + 2A_2 Q(\theta)c + \dots \quad (2)$$

where  $Q(\theta)$  is the interparticle interference factor and  $A_2$  is the second virial coefficient. The Zimm equation is obtained when  $Q(\theta)$  is set to be 1, since the Zimm equation is applicable to poor solvent systems, in which intermolecular interactions are weak and external interference is small.<sup>40,41</sup> Both  $P(\theta)$  and  $Q(\theta)$  reach 1 as  $\theta$  goes to zero, leading to the usual equation applicable to low-angle data:<sup>3</sup>

$$\frac{Kc}{R_0} = \frac{1}{M} + 2A_2 c + \dots \quad (3)$$

The data from standard PS are analyzed by these equations (eqs 2 and 3).

When the interactions are strong, as is the case of salt-free polyion solutions, more general relations than eqs 2 and 3 are needed to explain the behavior. We analyzed the concentration dependence of low-angle scattering data from ionomer solutions<sup>13,16</sup> by using Doty-Steiner equations, which were derived to analyze light scattering data from ionic hard spheres (e.g., bovine serum albumin).<sup>42</sup> These relations were derived from a general relation (eq 1) by using the Born-Green method<sup>43,44</sup> to include intermolecular interactions up to 3-body interactions. Although these equations were used by Doty and Steiner to analyze scattering data at

90° and the dissymmetry ratio ( $Z_{45} = R_{45}/R_{135}$ ), their approach may also be extended to interpret the angular dependence of the scattering for ionomer solutions.

To develop more general relations, the second bracketed term in eq 1 is written, by using the Born–Green method,<sup>43,44</sup> as

$$\left[1 + \frac{N}{V} \int_0^\infty \{1 - e^{-\psi(r)/kT}\} \frac{\sin(qr)}{qr} dv\right]^{-1} \quad (4)$$

where  $\psi(r)$  is the interparticle potential. Note the changes in signs by going from eq 1 to eq 4. Therefore, the reciprocal reduced scattered intensity is

$$\frac{Kc}{R_\theta} = \frac{1}{MP(\theta)} \left[1 + \frac{N}{V} \int_0^\infty \{1 - e^{-\psi(r)/kT}\} \frac{\sin(qr)}{qr} dv\right] \quad (5)$$

By choosing a proper potential function,  $\psi(r)$ , the reciprocal reduced scattered intensity,  $Kc/R_\theta$ , can be expressed for polyion solutions.<sup>42</sup> However, we can derive general relations without assuming any potential functions. To develop general relations,  $(\sin(qr))/qr$  in the brackets of eq 5 is expanded in a power series of  $qr$ , leading to the following equation:

$$\frac{Kc}{R_\theta} = \frac{1}{MP(\theta)} \left[1 + \frac{N}{V} \int_0^\infty \{1 - e^{-\psi(r)/kT}\} dv - \frac{q^2}{3!} \frac{N}{V} \int_0^\infty \{1 - e^{-\psi(r)/kT}\} r^2 dv + \dots\right] \quad (6)$$

The integrals in the brackets of eq 6 are the moments of  $\{1 - e^{-\psi(r)/kT}\}$ , which can be designated with the shorthand notation

$$m_n = \int_0^\infty \{1 - e^{-\psi(r)/kT}\} r^n dv \quad (7)$$

where  $m_n$  represents the  $n$ th moment. Especially important for our discussion are the following two moments:

$$m_0 = \int_0^\infty \{1 - e^{-\psi(r)/kT}\} dv \quad (7')$$

$$m_2 = \int_0^\infty \{1 - e^{-\psi(r)/kT}\} r^2 dv \quad (7'')$$

where  $m_0$  is considered to be the (intermolecular) excluded volume of the scatterer.<sup>3,45</sup> The ratio  $m_2/m_0$  ( $=\xi^2$ ) is considered to be a radius of gyration (mean-square radius) of the excluded volume, which is also a measure of the dimension of the region around a scattering particle, unoccupied by other particles (i.e., exclusion zones). By using these notations, eq 6 is now written as

$$\frac{Kc}{R_\theta} = \frac{1}{MP(\theta)} \left(1 + \frac{N}{V} m_0\right) \left[1 - q^2 \frac{\xi^2}{3!} \left(1 - \frac{1}{1 + \frac{N}{V} m_0} + \dots\right)\right] \quad (8)$$

At zero angle,

$$\frac{Kc}{R_0} = \frac{1}{M} \left(1 + \frac{N}{V} m_0\right) \quad (9)$$

Here,  $Kc/R_0$  is the reciprocal reduced scattered intensity at  $q = 0$  (zero angle limit), which is a function of  $c$ , initially increasing significantly and leveling off at

higher concentration, as already shown by low-angle scattering measurements for ionomer solutions.<sup>13,16</sup>

In addition, the particle scattering factor,  $P(\theta)$ , can be expressed, under the condition of  $qR_g < 1$ , as<sup>46</sup>

$$\frac{1}{P(\theta)} = 1 + \frac{R_g^2}{3} q^2 - \dots \quad (10)$$

where  $R_g$  denotes the radius of gyration of the scatterer (or the polymer coil) in contrast to  $\xi$ , the radius of gyration of the excluded volume (or exclusion zone) surrounding the polymer coil.

Finally, combining eqs 8–10, we can obtain an expression for the excess scattering from the solution of strongly interacting polymers:

$$\frac{Kc}{R_\theta} = \left(\frac{Kc}{R_0}\right) \left[1 + q^2 \left\{\frac{R_g^2}{3} - \frac{\xi^2}{6} \left(1 - \frac{R_0}{MKc}\right)\right\} - C'q^4\right] \quad (11)$$

Because both intramolecular and intermolecular scatterings are now expressed in a series of  $q^2$ , the following simple quadratic formula in  $q^2$  will be used for discussion:

$$\frac{Kc}{R_\theta} = b_0 + b_1 q^2 + b_2 q^4 \quad (12)$$

where the intercept,  $b_0 = Kc/R_0$ , is the reciprocal scattered intensity at zero angle. The initial slope normalized against the intercept,  $b_1/b_0$ , is

$$\frac{b_1}{b_0} = \frac{R_g^2}{3} - \frac{\xi^2}{6} \left(1 - \frac{R_0}{MKc}\right) \quad (13)$$

Note that, in the case of no intermolecular interference ( $\xi = 0$ ) or zero concentration limit ( $MKc/R_0 = 1$ ), the normalized slope,  $b_1/b_0$ , is simply the true radius of gyration of the scatterer. At finite concentrations, we can regard this  $b_1/b_0$  value as the square of the *apparent* radius of gyration ( $R_{g,app}^2/3$ ), since the second term in eq 13 cannot be ignored. It is seen from eq 13 that the normalized slope can even be negative if the negative contribution of the second term is large, as is the case of polyion at low polymer concentrations. Experimentally, the  $b_1/b_0$  term in eq 13 is determined from angular data and the  $R_0/MKc$  term is determined from low-angle data (or angular data extrapolated to zero angle).

It should be stressed that in this derivation we consider triplet terms at least to a first approximation in addition to pair terms by using the Born–Green method, as pointed out by Guinier and Fournet.<sup>47,48</sup> Somewhat similar relations have been used by Burchard to analyze light scattering data for poly(vinylcarbazole) solution, where ordering of polymer molecules occurs due to large excluded volume, presumably arising from solvation.<sup>51</sup> Note that these equations are quite general; it is not difficult to show that eqs 2 and 3 are special cases of eqs 8 and 9, respectively.

## Results

Figure 3 shows the light scattering results for SPS ionomer with various ion contents in DMF: the scattering data by angular measurements, extrapolated to zero angle, are shown in addition to low-angle scattering data. The result for the starting polystyrene is also included for comparison. It is seen that the reciprocal

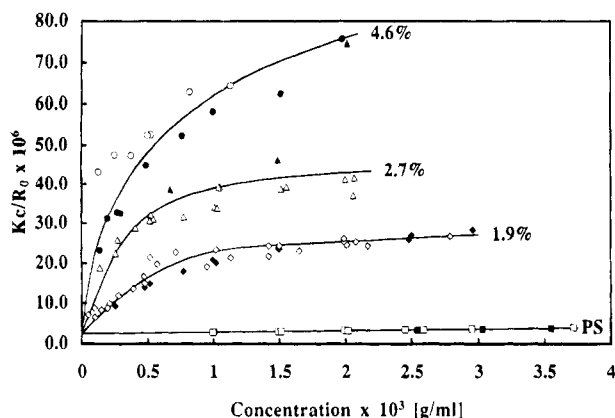


**Figure 3.** Reciprocal reduced scattered intensity at zero angle,  $Kc/R_0$ , for SPS ionomer with various ion contents in DMF as well as polystyrene: closed symbols, low-angle light scattering data; open symbols, angular light scattering data extrapolated to zero angle.

reduced scattered intensity,  $Kc/R_0$ , from ionomer solutions rises steeply from the intercept, bends over, and becomes nearly horizontal at higher polymer concentrations. Furthermore, the curves for ionomer samples with different ion contents seem to converge to the same intercept at zero concentration, corresponding to the inverse of the weight-average molecular weight of the polymer. These are consistent with the results reported for SPS ionomers in DMF<sup>13,15,17</sup> and for polyelectrolytes in aqueous solution.<sup>28,42,52</sup> It should be noted that there is a good agreement between low-angle data and angular scattering data extrapolated to zero angle, which were obtained by independent instruments, indicating the reliability of our light scattering experiments.

Figure 4 shows a Zimm plot for the SPS ionomer in DMF. It should be stressed that the reproducibility of the data, especially that of the low-concentration range, is very good, since these data were collected by seven independent experiments using different stock solutions. As explained above, an extrapolated curve to zero angle (line connecting open squares) is quite close to that obtained by low-angle light scattering measurements. The most noteworthy feature in this figure is the negative slope of the angular-dependent curves for low-concentration solutions, as shown in Figure 4b. This reflects the fact that the reciprocal reduced scattered intensity increases with increasing scattering angle, which is opposite to that seen for neutral polymer solution, where the slope is always positive, as seen in Figure 2. As the ionomer concentration is increased, the slope in the angular-dependent curve increases with increasing polymer concentration and eventually becomes positive, somewhat curved at low angles, as seen in Figure 4a. Due to this curvature, we used a quadratic relation (eq 12) for fitting the data and determined the zero-angle value,  $b_0$ , and the initial slope,  $b_1$ . Although the  $b_2$  value was also obtained, this is a complex function of moments higher than the second (i.e.,  $\xi$  and  $R_g$ ).

To show more clearly the concentration dependence of each angular-dependent curve in Figure 4a, the values of the normalized slope,  $b_1/b_0$ , are plotted against polymer concentration in Figure 5. It is seen that, as the polymer concentration increases, the value of the normalized slope changes from largely negative, to less negative, and eventually to slightly positive.

To show that this characteristic behavior of the salt-free ionomer solution arises from ionic interactions, light scattering measurements were also conducted for ionomer solutions with added salts (0.1 M  $\text{NaNO}_3$ ); since

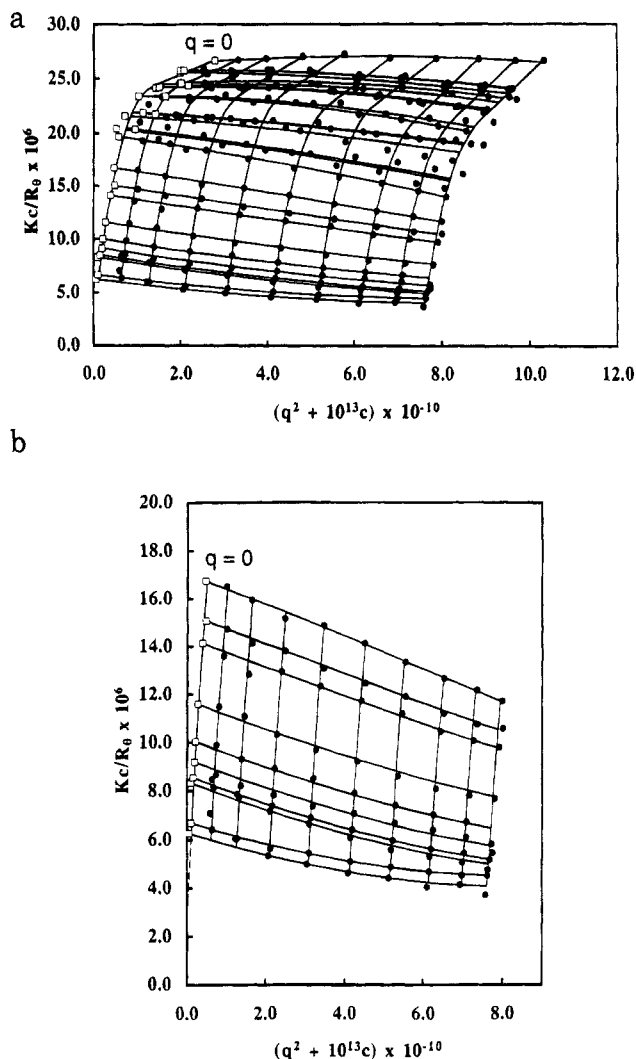


**Figure 4.** (a) Overall Zimm plot of ionomer (ion content: 1.9 mol %) in DMF. (b) Zimm plot at low concentrations of ionomer (ion content: 1.9 mol %) in DMF: closed symbols, experimental values; open symbols, extrapolated values.

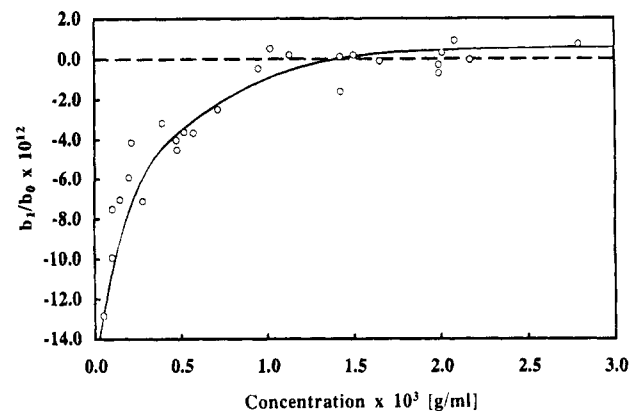


**Figure 5.** Normalized initial slope in  $Kc/R_0$  vs  $q^2$  curves,  $b_1/b_0$ , against ionomer concentration for ionomer (ion content: 1.9 mol %) in DMF.

simple salts can suppress ionic interactions by screening ionomer charges, neutral polymer behavior should be recovered, as observed for viscosity and low-angle light scattering data, if this characteristic behavior arises from ionic interactions.<sup>14</sup> It was found that the addition of simple salts indeed suppressed the characteristic behavior both in low-angle light scattering behavior (i.e., a significant reduction in scattered intensity) and in angular light scattering behavior (i.e., an increased

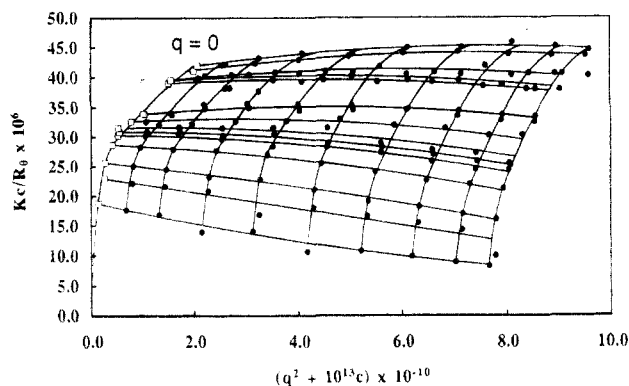


**Figure 6.** Zimm plot for ionomer (ion content: 2.7 mol %) in DMF: closed symbols, experimental values; open symbols, extrapolated values.

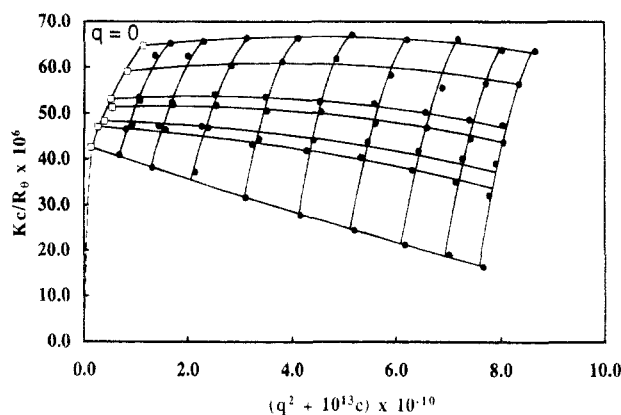


**Figure 7.** Zimm plot for ionomer (ion content: 4.6 mol %) in DMF: closed symbols, experimental values; open symbols, extrapolated values.

scattered intensity with increasing scattering angle at low concentration).

The effect of ion content on "abnormal" Zimm plots is seen in Figures 6 and 7 for the higher ion content samples (2.7 and 4.6 mol %). The slope of the angular-dependent curve (i.e.,  $Kc/R_\theta$  vs  $q^2$  curves) is negative at low concentration and becomes less negative and eventually positive as ionomer concentration increases. Both systems show similar results to those seen for the 1.9 mol % ionomer, but in a more pronounced fashion. This is yet another example of salt-free polyelectrolyte behavior of ionomer solutions, in which the degree of polyelectrolyte effect increases with increasing ion content.<sup>5</sup>

Figure 8 shows the concentration dependence of the normalized initial slope,  $b_1/b_0$ , for the ionomers with three different ion contents (1.9, 2.7, and 4.7 mol %) to show the effect of ion content. It is apparent that the  $b_1/b_0$  values at both low and high concentrations are more pronounced as the ion content increases. Furthermore, the crossover concentration, where the initial slope changes from negative to positive, shifts to lower concentration as the ion content is increased.

## Discussion

In this work, we have shown characteristic light scattering behavior (angular dependence) of SPS ionomers in a polar solvent, DMF; at low ionomer concentration, an angular-dependent curve shows a negative slope, the slope increases with increasing ionomer concentration, and eventually it becomes positive at high ionomer concentration. Since a contrasting behavior is observed according to the concentration range,

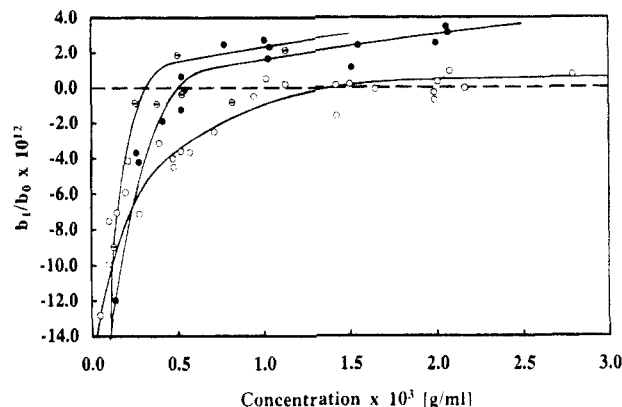


**Figure 8.** Normalized initial slope in  $Kc/R_\theta$  vs  $q^2$  curves,  $b_1/b_0$ , for ionomers with various ion contents in DMF. (○) 1.9 mol %; (●) 2.7 mol %; (⊙) 4.6 mol %.

we divide the concentration range into two ranges for discussion: one is the low-concentration range, where the slope is negative, and the other is the high-concentration range, where the slope is positive. The crossover concentration is designated as  $c^+$  in this paper.<sup>53</sup>

**Low Concentrations.** Although our results are most systematic, demonstrating the negative slope of the angular-dependent curve, some previous work suggested a similar behavior: for example, Doty and Steiner reported that the dissymmetry ratio ( $R_{45}/R_{135}$ ) of bovine serum albumin (a charged protein) in water was less than 1, indicating that the scattering at high angle was stronger than at low angle.<sup>42</sup> It was also reported for salt-free polyelectrolytes in water that the reciprocal scattered intensity at low concentration decreased with increasing scattering angle for sodium poly(styrenesulfonate) by Sedlak and Amis<sup>54</sup> and for poly(2-vinylpyridine) (PVP) (quaternized) by Förster et al.,<sup>55</sup> although their data were reported in normalized reciprocal scattered intensity,  $I_0/I_\theta$ , instead of reciprocal reduced scattered intensity,  $Kc/R_\theta$ , usually used for light scattering data analysis. As we previously noted,<sup>13</sup> the excess scattering from ionomers in a polar solvent is much stronger than that from polyelectrolytes with comparable molecular weight in aqueous solution; therefore, the relative error in scattering data from ionomer solution is smaller compared with polyelectrolyte solution. Thus, we can say with more confidence that these curves are characteristic to ionic polymers in polar solvents, including polyelectrolytes in aqueous solution. Probably, most relevant is the result reported by Sakamoto et al. for PVP (unquaternized) in methanol:<sup>56</sup> here, also, "abnormal" light scattering behavior, such as negative slopes, was observed for PVP in methanol. Although they correctly attributed this "abnormal" behavior to external interference arising from nonrandom arrangement of polymer molecules, this arrangement was attributed to a strong solvation and resulting increased repulsion between polymer molecules. However, they also pointed out that the addition of HCl to methanol, which can lead to partial ionization of PVP molecules, enhanced "abnormality" in light scattering behavior. This suggests that the strong ionic interaction arising from partial ionization is the cause of abnormality, as we observe in ionomer solutions, since partially ionized PVP may be much closer to ionomers of low ion content. As we indicated, the introduction of very small amounts of ionic groups (e.g., 1 mol %) can induce polyelectrolyte behavior.<sup>16</sup>

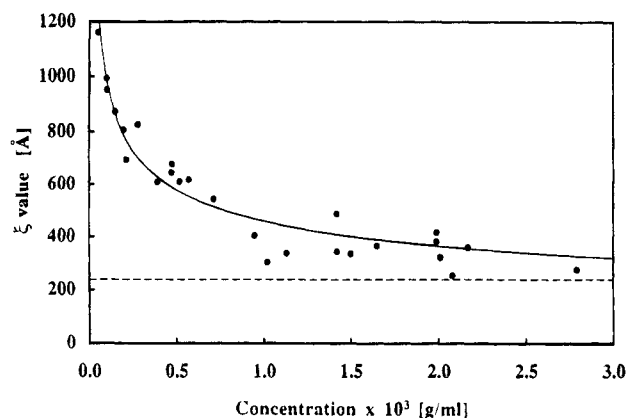


**Figure 9.** Radius of gyration of excluded volume,  $\xi$ , vs ionomer concentration for ionomer (ion content: 1.9 mol %) in DMF. Dashed line represents the radius of gyration,  $R_g$ , of unmodified polystyrene.

This characteristic scattering behavior of ionomer solutions may be analyzed by using the equations developed above. As eq 13 indicates, the normalized initial slope (or apparent radius of gyration) term,  $b_1/b_0$ , is considered to arise from the competition between the first term,  $R_g^2/3$ , reflecting the radius of gyration of ionomer chains (therefore a positive contribution), and the second term,  $(-\xi^2/6)(1 - R_0/MKc)$ , reflecting the excluded volume (therefore a negative contribution). However, as the neutron scattering experiments have shown, the increase in the radius of gyration of the SPS ionomer chain with decreasing ionomer concentration is rather small,<sup>19,57</sup> and therefore, to a first approximation, the change in  $R_g$  of the ionomer chain is negligible compared with that of  $\xi$  over the concentration range studied. Therefore, the change in the  $b_1/b_0$  value (or normalized slope) can be discussed in terms of the change in the excluded volume term (the second term in eq 13). Figure 9 shows the concentration dependence of  $\xi$  values calculated from eq 13 with the assumption of constant  $R_g$ . The  $R_g$  value for unmodified polystyrene (i.e., 239 Å) was used for calculation. As expected, the radius of gyration of the excluded volume,  $\xi$ , decreases with increasing ionomer concentration.

We can now understand the concentration dependence of the  $b_1/b_0$  term in Figure 5: at low concentration, the value is negative, reflecting the dominant excluded volume term, because ionomer molecules have a large excluded volume due to long-range electrostatic interactions between molecules, as seen in Figure 9. As the ionomer concentration increases, the total ionic strength of the solution increases, thereby reducing the intermolecular electrostatic interactions. Thus, the electrostatic excluded volume term  $\xi$  decreases significantly (see Figure 9), while  $(1 - R_0/MKc)$  increases slightly (see Figure 3), leading to a small negative value. The slope is still negative, because the radius of gyration of ionomer chains is much smaller than the excluded volume term as far as ionomer concentration is low (see Figure 9). This is in contrast to the case of neutral polymer solutions, where the intermolecular interactions are short range (e.g., van der Waals interactions); thus, the excluded volume is of the same order of  $R_g^3$ , and hence  $\xi$  as well as  $(1 - R_0/MKc)$  is small, leading to a positive slope. However, even in neutral polymer solutions, the presence of the excluded volume term can be seen in the scattering data: the slope of  $Kc/R_\theta$  vs  $q^2$  plots decreases with increasing polymer concentration.<sup>39,58</sup> This is because as concentration is increased,  $(1 - R_0/MKc)$  increases, and thereby the importance of

the  $(-\xi^2/6)(1 - R_0/MKc)$  term also increases (the  $\xi$  value is considered to be roughly constant for neutral polymers).

It has been shown that the polyelectrolyte effect of ionomer solutions becomes more pronounced as the ion content is increased.<sup>5,16</sup> Therefore, an increase in ion content should have two opposing effects on the slope of the  $Kc/R_\theta$  vs  $q^2$  curve. First, the electrostatic interactions will become stronger due to a larger number of ions on the chain, leading to larger electrostatic excluded volume. Therefore,  $\xi$ , as well as  $(1 - R_0/MKc)$  in eq 13, increases, resulting in a more negative contribution to the  $b_1/b_0$  term. Second, chain expansion may be more pronounced, leading to a more positive contribution to the  $b_1/b_0$  term. However, the change in  $R_g$  is less significant<sup>19,57</sup> compared with that of  $\xi$ . At best,  $R_g$  can scale with ion content in a similar degree to  $\xi$ . Therefore, an increase in ion content leads to a larger negative contribution than a positive one in eq 13, thereby producing more pronounced negative slopes, as seen in Figures 6 and 7.

We can also show that the crossover concentration,  $c^+$ , where the normalized slope ( $b_1/b_0$ ) becomes zero, shifts to lower concentration with increasing ion content.<sup>53</sup> Qualitatively, it is expected that higher ion content leads to larger excluded volume, leading to a larger contribution of the  $\xi$  term compared with the  $R_g$  term in eq 13, as discussed above; therefore, the crossover concentration shifts to lower concentration. More quantitatively, from eqs 9 and 13, the crossover concentration is obtained as

$$c^+ \sim \frac{1}{m_0} \left( \frac{\xi^2}{2R_g^2} - 1 \right)^{-1} \quad (14)$$

under the condition that  $MKc/R_0 \gg 1$ , which is the case for ionomer solutions at relatively high concentration where the crossover occurs, as seen in Figure 3. The higher the ion content, the larger the excluded volume  $m_0$ , and  $R_g$  and  $\xi$  can scale with ion content in a similar degree at best; actually, the change in  $\xi$  is much larger than that of  $R_g$ , as already discussed. Therefore,  $c^+$  shifts to lower concentration with ion content.

**High Concentrations.** At higher concentrations, the slope of the angular-dependent curve becomes positive, somewhat curved at lower angles, indicating that the first term in eq 13, reflecting the radius of gyration of the polymer, dominates. While the apparent radius of gyration of the 1.9 mol % ionomer is comparable to that of the unmodified polystyrene (239 Å) over the concentration range studied, the higher ion content samples (2.7 and 4.6 mol %) show larger values; for example, the values of apparent radius of gyration for these samples are over 300 Å. However, a true radius of gyration is even larger compared with such an apparent radius of gyration because of the excluded volume term (i.e., the second term) in eq 13. In addition, the appearance of the curvature at small angles suggests the existence of larger particles in the solution, as observed for a solution of heterogeneous samples (in terms of size).<sup>59</sup>

These considerations suggest the existence of "heterogeneities" that are larger than the parent polystyrene. It should also be noted that the apparent radius of gyration increases with increasing ion content at high concentration (see Figure 8). This again indicates that the "heterogeneities" in the solution become more pronounced with increasing ion content, suggesting that



the phenomenon is ionic in nature. It should be added that the CONTIN analysis of dynamic scattering data for the SPS ionomers in DMF indicates the existence of two diffusive modes: a fast mode and a slow mode. The slow mode may reflect the scattering from these large "heterogeneities".<sup>60</sup>

The solution is considered to be made of ionomer chains surrounded by a large exclusion zone. It is expected that the effective volume of each ionomer chain begins to overlap at high concentration. This concentration should be much lower for the ionomer compared with unmodified polystyrene. For example, the effective (or excluded) volume of 1.9 mol % ionomer at high concentration is nearly 10 times larger than that of polystyrene. This can be seen in the ca. 10 times larger  $Kc/R_0$  value of the 1.9 mol % sample compared with polystyrene at  $1.5 \times 10^{-3}$  g/cm<sup>3</sup>, as seen in Figure 3 (also see eq 9). Therefore, this leads to a decrease in the critical concentration where overlap of the effective volume occurs. An analogy may be found in the condensation of a gas (polymer molecules at low concentration) to a liquid (dense arrangement of polymer molecules) with a decrease in specific volume (increase in polymer concentration), except that the effective volume of the ionomer molecule decreases with concentration, while that of the gas molecule is constant. The "heterogeneities" may reflect larger species formed due to the fluctuation of particle position at this critical concentration.

It should be mentioned that somewhat similar light scattering behavior was reported for salt-free polyelectrolyte solutions; a pronounced positive slope has been reported in the angular light scattering data from polyelectrolytes (sodium poly(styrenesulfonate)<sup>54</sup> and quaternized PVP<sup>55</sup>) in water at high concentrations. These results, coupled with the dynamic light scattering results, have been interpreted as arising from large-scale "domains" in the solution.<sup>61</sup> Some explanations have been proposed to explain the formation of "domains" in salt-free polyion solutions. One explanation is offered by Ise et al.<sup>62</sup> They attributed the origin of such behavior to attractive interaction between different polyions through intermediary counterions with opposite sign. In their "two-state model", both free polyions and associated species (corresponding to a "domain") coexist in the solution. Another is the so-called temporal aggregate model by Schmitz et al.,<sup>63,64</sup> which explains the formation of "domains" due to dipole-dipole type attractions through the distortion of counterion clouds. However, there are some arguments against the existence of "domains".<sup>65</sup> It should also be added that even neutral polymers in good solvent as well as polyelectrolytes with added salts show similar angular light scattering results at high concentration.<sup>59,66,67</sup> Certainly, no attraction due to ionic interactions is expected for the neutral polymer solutions.

It is not our intention in this paper, however, to identify the origin of "heterogeneities" formed in salt-free ionomer solutions. More systematic studies to characterize the "heterogeneities" and experiments targeted to separate the essential factor causing the behavior are needed. Future studies will address these issues. Nevertheless, we have shown that ionomer solutions clearly show characteristic light scattering behavior, such as negative angular dependence at low concentration and positive slope with some curvature at high concentration, which have been only partly

indicated before by angular light scattering studies for salt-free polyelectrolyte solutions.

## Conclusions

Angular light scattering measurements were conducted for sulfonated polystyrene ionomers, in which small amounts (less than 5 mol %) of ionic groups were randomly distributed, dissolved in an aprotic, polar solvent, DMF. The angular light scattering results extrapolated to zero angle are in good agreement with low-angle light scattering results from the same system. The data show a decrease in reciprocal reduced scattered intensity with increasing scattering angle at low polymer concentrations, which is explained in terms of the large (intermolecular) excluded volume of ionomer molecules. At higher concentrations, reciprocal reduced scattered intensity increases with scattering angle, and a slight curvature is seen at small angles, which is characteristic of a solution with large-scale "heterogeneities". The presence of large scale "heterogeneities" found for ionomer solutions is similar to those reported for salt-free polyelectrolyte solutions, whose structure and origin are still controversial. Because of the stronger scattering power and nonaqueous nature of ionomer solutions compared with polyelectrolytes in aqueous solution, salt-free ionomer solutions can be used as a good model system to investigate the characteristic behavior of salt-free polyelectrolyte solutions. The use of simpler ionomer systems, such as smaller random ionomers (to eliminate the  $R_g$  term contribution, arising from intramolecular interference) and telechelic ionomers with a single charge per chain (to eliminate the effect of intramolecular electrostatic interactions) can further clarify some of the unanswered questions. These studies are underway and will be reported in the future.

**Acknowledgment.** We would like to acknowledge the NSF for partial support of this research.

## References and Notes

- (1) Nagasawa, M.; Takahashi, A. In *Light Scattering from Polymer Solutions*; Huglin, M. B., Ed.; Academic Press: New York, 1972; Chapter 16.
- (2) Mandel, M. In *Polyelectrolytes: Science and Technology*; Hara, M., Ed.; Marcel Dekker: New York, 1993; Chapter 1.
- (3) Yamakawa, H. *Modern Theory of Polymer Solutions*; Harper and Row: New York, 1971.
- (4) de Gennes, P.-G. *Scaling Concepts in Polymer Physics*; Cornell University Press: Ithaca, NY, 1979.
- (5) Hara, M. In *Polyelectrolytes: Science and Technology*; Hara, M., Ed.; Marcel Dekker: New York, 1993; Chapter 4.
- (6) Holliday, L., Ed. *Ionic Polymers*; Applied Science: London, 1975.
- (7) Eisenberg, A.; King, M. *Ion Containing Polymers*; Academic: New York, 1977.
- (8) MacKnight, W. J.; Earnest, T. R. *J. Polym. Sci., Macromol. Rev.* **1981**, *16*, 41.
- (9) Lundberg, R. D.; Phillips, R. R. *J. Polym. Sci., Polym. Phys. Ed.* **1982**, *20*, 1143.
- (10) Pedley, A. M.; Higgins, J. S.; Peiffer, D. G.; Burchard, W. *Macromolecules* **1990**, *23*, 1434.
- (11) Gabrys, B.; Higgins, J. S.; Lantman, C. W.; MacKnight, W. J.; Pedley, A. M.; Peiffer, D. G.; Rennie, A. R. *Macromolecules* **1989**, *22*, 3746.
- (12) Rochas, C.; Domard, A.; Rinaudo, M. *Polymer* **1979**, *20*, 76.
- (13) Hara, M.; Wu, J. *Macromolecules* **1986**, *19*, 2887.
- (14) Hara, M.; Wu, J.; Lee, A. H. *Macromolecules* **1989**, *22*, 754.
- (15) Lantman, C. W.; MacKnight, W. J.; Peiffer, D. G.; Sinha, S. K.; Lundberg, R. D. *Macromolecules* **1987**, *20*, 1096.
- (16) Hara, M.; Wu, J. *Macromolecules* **1988**, *21*, 402.
- (17) Hara, M.; Wu, J.; Jerome, R. J. *Macromolecules* **1988**, *21*, 3330.
- (18) Wu, J.; Wang, Y.; Hara, M.; Granville, M.; Jerome, R. *Macromolecules* **1994**, *27*, 1195.



- (19) Lantman, C. W.; MacKnight, W. J.; Sinha, S. K.; Peiffer, D. G.; Lundberg, R. D.; Wignall, G. D. *Macromolecules* **1988**, *19*, 1344.
- (20) Aldebert, P.; Dreyfus, B.; Pineri, M. *Macromolecules* **1986**, *19*, 2651.
- (21) Wang, J.; Wang, Z.; Peiffer, D. G.; Shuely, W. J.; Chu, B. *Macromolecules* **1991**, *24*, 790.
- (22) Hara, M.; Wu, J. *ACS Symp. Ser.* **1989**, *395*, 446.
- (23) Wu, J. L.; Hara, M. *Macromolecules* **1994**, *27*, 923.
- (24) Kupperblatt, G.; Hara, M. *Macromolecules*, to be submitted.
- (25) Oosawa, F. *Polyelectrolytes*; Marcel Dekker: New York, 1971.
- (26) Rice, S. A.; Nagasawa, M. *Polyelectrolyte Solutions*; Academic Press: New York, 1961.
- (27) Hara, M., Ed. *Polyelectrolytes: Science and Technology*; Marcel Dekker: New York, 1993.
- (28) Oth, A.; Doty, P. *J. Phys. Chem.* **1952**, *56*, 43.
- (29) Drifford, M.; Dalbiez, J. P. *J. Phys. Chem.* **1984**, *88*, 5368.
- (30) (a) Tabor, B. E. In *Light Scattering from Polymer Solutions*; Huglin, M. B., Ed.; Academic Press: New York, 1972; Chapter 1. (b) It was reported<sup>30c</sup> that poly(styrenesulfonic acid) showed a sign of decomposition under ambient conditions. However, there is little sign of such changes for SPS copolymer even after several years of storage in this laboratory. (c) Reddy, M.; Marinsky, J. A. *J. Phys. Chem.* **1970**, *74*, 3884.
- (31) Hara, M.; Wu, J.; Lee, A. H. *Macromolecules* **1988**, *21*, 2214.
- (32) Hara, M.; Lee, A. H.; Wu, J. *J. Polym. Sci., Polym. Phys. Ed.* **1987**, *25*, 1407.
- (33) Makowski, H. S.; Lundberg, R. D.; Singhal, G. H. US Patent 3870841, 1975 (assigned to Exxon Research and Engineering Co.).
- (34) Kaye, W.; Havlik, A. J. *Appl. Opt.* **1973**, *12*, 541.
- (35) Thurmond, C. D. *J. Polym. Sci.* **1952**, *8*, 607.
- (36) Kaye, W.; McDaniel, J. B. *Appl. Opt.* **1974**, *13*, 1934.
- (37) Berry, G. C. *J. Chem. Phys.* **1966**, *44*, 4550.
- (38) Zernicke, F.; Prins, J. Z. *Phys.* **1927**, *41*, 184.
- (39) Flory, P. J.; Bueche, A. M. *J. Polym. Sci.* **1958**, *27*, 219.
- (40) Zimm, B. H. *J. Chem. Phys.* **1948**, *16*, 1093.
- (41) Zimm, B. H. *J. Chem. Phys.* **1948**, *16*, 1099.
- (42) Doty, P.; Steiner, R. F. *J. Chem. Phys.* **1952**, *20*, 85.
- (43) Born, M.; Green, M. *Proc. R. Soc. London* **1946**, *A188*, 10.
- (44) Fournet, G. *Acta Crystallogr.* **1951**, *4*, 293.
- (45) Flory, P. J. *Principles of Polymer Chemistry*; Cornell University Press: Ithaca, NY, 1953.
- (46) Debye, P. *J. Phys. Colloid. Chem.* **1947**, *51*, 18.
- (47) Guinier, A.; Fournet, G. *Small-Angle Scattering of X-rays*; John Wiley: New York, 1955.
- (48) More general relations to accommodate many-body interactions may be obtained by using Percus-Yevick equations,<sup>49</sup> as shown by Vrij.<sup>50</sup> However, the treatment of Fournet is sufficient for our discussion.
- (49) Percus, J. K.; Yevick, G. J. *Phys. Rev.* **1958**, *110*, 1.
- (50) Vrij, A. *J. Chem. Phys.* **1978**, *69*, 1742.
- (51) Burchard, W. *Polymer* **1969**, *10*, 29.
- (52) Trap, J. J. L.; Hermans, J. J. *J. Phys. Chem.* **1954**, *58*, 757.
- (53) The overlap concentration  $c^*$ , is usually defined as the concentration where each polymer begins to overlap. In contrast, the crossover concentration, defined here as  $c^+$ , seems to close to the critical concentration where the "effective" volume of the polymer chain begins to overlap.
- (54) Sedlak, M.; Amis, E. J. *J. Chem. Phys.* **1992**, *96*, 826.
- (55) Förster, S.; Schmidt, M.; Antonietti, M. *Polymer* **1990**, *31*, 781.
- (56) Sakamoto, N.; Yoshida, M.; Arichi, S. *Bull. Chem. Soc. Jpn.* **1974**, *47*, 1363.
- (57) Weill, G. *Biophys. Chem.* **1991**, *41*, 1.
- (58) This is equivalent to say that  $Q(\theta)$  in eq 2 is a decreasing function of  $c$ .
- (59) Huglin, M. B. *Light Scattering from Polymer Solutions*; Academic Press: New York, 1972.
- (60) Bodycomb, J.; Hara, M. *Macromolecules*, submitted.
- (61) Sedlak, M. *Macromolecules* **1993**, *26*, 1158.
- (62) Ise, N. *Angew. Chem., Int. Ed. Engl.* **1986**, *25*, 323.
- (63) Schmitz, K. S.; Lu, M.; Singh, N.; Ramsay, D. J. *Biopolymers* **1984**, *23*, 1637.
- (64) For a discussion of ordering in polyelectrolyte solution, see: Schmitz, K. S. *Dynamic Light Scattering by Macromolecules*; Academic Press: San Diego, CA, 1990; pp 383-390.
- (65) Reed, W. F. *Macromolecules* **1994**, *27*, 873.
- (66) Hara, M.; Nakajima, A. *Polym. J.* **1980**, *12*, 693.
- (67) Hara, M.; Nakajima, A. *Polym. J.* **1980**, *12*, 703.